

Modeling the Charge State of Monatomic Hydrogen and Other Defects with Arbitrary Concentrations in Crystalline Silicon

Chang Sun,* Di Yan, and Daniel Macdonald


A rigorous physical-mathematical model for predicting the charge states of both mono- and multivalent defects with arbitrary concentrations in Si in both thermal equilibrium and non-equilibrium steady-state conditions is presented. The model avoids the assumption that the defect concentration is much lower than the doping level, which is common in previous approaches. It is shown that the general occupancy ratio given by $\alpha = (kn_1 + p)/(kn + p_1)$ is still valid under these more general conditions. However, more caution needs to be taken when calculating the equilibrium and excess carrier densities in the presence of larger defect concentrations, because of: a) the non-negligible contribution to n_0 and p_0 from defect ionisation, and b) unequal Δn and Δp caused by the change in the occupied states at the defect level from equilibrium to non-equilibrium. Modeled examples of monatomic H and interstitial Fe in Si are shown and the effects of defect concentration, temperature, and carrier injection are discussed.

1. Introduction

Knowledge of the charge states of monatomic hydrogen (H), and other deep-level defects in Si, has been found to be crucial in understanding the prevailing forms^[1,2] and transport^[3,4] of H in Si, the interactions between H and dissolved transition metals in Si,^[5–11] as well as other point-defect reactions in Si.^[12–15] A unified model for predicting the charge states of H and other deep-level defects in Si was described in our previous works.^[16,17] Four models in the literature 1) the Fermi distribution, 2) the Shockley–Last model,^[18] 3) the Shockley–Read–Hall (SRH) model,^[19,20] and 4) the Sah–Shockley model^[21] were summarized by the general occupancy ratio, which was demonstrated to universally apply to the charge state prediction of both mono- and multivalent defects in both thermal equilibrium and non-equilibrium steady-state conditions.^[16]

C. Sun, D. Macdonald
School of Engineering
The Australian National University
Canberra, ACT 2601, Australia
E-mail: chang.sun@anu.edu.au

D. Yan
Department of Electrical and Electronic Engineering
The University of Melbourne
Melbourne, Victoria 3010, Australia

 The ORCID identification number(s) for the author(s) of this article can be found under <https://doi.org/10.1002/pssr.202100483>.

DOI: 10.1002/pssr.202100483

It was also pointed out in our previous work^[16] that the quasi-Fermi level approximations, which were sometimes applied to deep levels for the charge state estimation under injection in some studies,^[13,14,22,23] should theoretically be avoided. The split electron and hole quasi-Fermi levels are a natural solution of the dilemma that the increased electron/hole densities under injection can only be described by separate Fermi levels closer to the conduction/valence bands.^[24] However, for deep levels in the bandgap, neither quasi Fermi level applies; the occupation of states at the deep levels is rather determined by the kinetics of the capture and emission of the carriers,^[24] which was systematically considered by the SRH statistics for monovalent defects,^[19,20] and by Sah and

Shockley for multivalent defects,^[21] as discussed in the previous work.^[16] Results from two experimental studies have now shown that the unified model based on the kinetics^[16] gives more reliable predictions than the quasi-Fermi level approximations. In a study by Mullins et al.,^[10] a large fraction of monatomic H was found to be positively charged in p-type Si (p-Si) with $[B^-] \approx 2 \times 10^{15} \text{ cm}^{-3}$ and $\Delta n \approx 7 \times 10^{15} \text{ cm}^{-3}$ at 110 °C, by combining reverse bias annealing and capacitance-voltage (CV) measurements of active doping. Under this condition, the unified model predicts $\approx 80\%$ H to be positively charged, while the electron quasi-Fermi level approximation predicts $>99\%$ H atoms negatively charged. In the second study,^[15] the dissociated fraction of FeB pairs in p-Si with $[B^-] = 1.4 \times 10^{15} \text{ cm}^{-3}$ was experimentally determined to be 10–80% under different injection levels from $4 \times 10^{12} \text{ cm}^{-3}$ to $4 \times 10^{13} \text{ cm}^{-3}$ at 296 K. Contradicting this, the electron quasi-Fermi level approximation predicts $>95\%$ pairs to be dissociated under an injection level as low as 10^{11} cm^{-3} .

An important assumption in the previous model is that the defect concentration is much lower than the doping level. This assumption originated from the simplified SRH model,^[19] and is realistic under most circumstances. However, it does not always hold, a most common exception being the monatomic H in silicon wafers after a hydrogenation treatment. For example, the CV measurements by Mullins et al.^[10] indicated that, the monatomic H that binds to B was in a similar order of magnitude as $[B^-] = 2 \times 10^{15} \text{ cm}^{-3}$, in the first 5 μm from the surface after remote hydrogen plasma treatment and annealing. In Kleekajai et al.'s work,^[25] infrared spectroscopy measurements showed

that the total hydrogenated Pt impurities after a fast firing process with SiN_x:H coatings were $\approx 10^{15} \text{ cm}^{-3}$. The total hydrogen concentration in Si has also been measured in the literature, showing that the total hydrogen concentration can easily exceed the doping level, although how much of it exists as monatomic H is usually more difficult to determine. In Walter et al.'s work,^[26] the total hydrogen concentration in the wafer bulk after a fast firing process with SiN_x:H coatings was estimated to be in the 5×10^{14} – $1.3 \times 10^{15} \text{ cm}^{-3}$ range, via measuring resistivity changes after intentional formation of B-H pairs. In Wenham et al.'s work,^[27] the total hydrogen concentration in 1.4 μm from the surface in a heavily doped poly-Si layer after hydrogen plasma exposure, was determined to be in the 10^{19} – 10^{21} cm^{-3} range by secondary ion mass spectrometry (SIMS) analysis. The heavy doping concentration [B] or [P] was exceeded by the total hydrogen concentration by approximately three orders of magnitude.

Therefore, a more general model avoiding the previous assumption, that is, a model for defects with arbitrary concentrations, is required for the charge state prediction under such circumstances. This problem was already considered in Shockley and Read's work,^[19] known as the general SRH model, in contrast to the simplified SRH model requiring the assumption.^[28] However, how to determine the equilibrium carrier densities in the presence of a significant defect concentration was not shown. The problem was also considered by Chen et al.^[29] using an iterative algorithm that finds the convergent equilibrium carrier densities for a given doping level, defect concentration and excess carrier density. The model remains highly numerical without the physics being thoroughly discussed, and in addition, the effect of the defect concentration on excess carrier densities was missing. A complete set of equations solving the problem was presented in a study by McIntosh et al.,^[30] but as the study was heavily orientated to modeling the recombination lifetime, the charge state prediction was scarcely discussed. In this work, we intend to present a rigorous physical-mathematical model for the charge state prediction of defects with arbitrary concentrations in Si. The model is based on the general SRH model,^[19,28] but extends it to both mono- and multivalent defects in both thermal equilibrium and non-equilibrium steady-state conditions.

We will discuss the physics and modeling results with two examples: the interstitial Fe (Fe_i)—a single donor,^[31] and the monatomic H—a negative-U defect^[1,32] (introducing both a donor and an acceptor level, with the donor located above the acceptor in the bandgap). **Table 1** shows the assumed energy levels and the capture cross section ratios of Fe_i and H. The capture cross section ratios of H were estimated by assuming that the H deep levels follow the trend in the capture cross section ratios of point-like transition-metal impurities in Si in the previous model.^[16] We will explain the methodology for the monovalent

Fe_i in full detail, and then explain more concisely how the model for multivalent defects can be built in an analogical way on the basis of the Fe_i model. The occupancy ratio defined in the previous work^[16] will be kept in use in this work: an energy level $E(s + 1/2)$ introduced by a mono-/multivalent defect, is associated with two charge states: s (when occupied by a hole), and $s + 1$ (when occupied by an electron). The occupancy ratio is the ratio of the defect concentration in charge state s to that in charge state $s + 1$.

2. Model

2.1. Thermal Equilibrium

The expression for the thermal occupancy ratio for monovalent defects based on the Fermi distribution, and for multivalent defects based on the Shockley–Last model, is theoretically not affected by the defect concentration.^[16,18,24] For Fe_i, it is

$$\frac{[\text{Fe}_i^+]_0}{[\text{Fe}_i^0]_0} = \frac{p_0}{p_1} = \frac{n_1}{n_0} \quad (1)$$

where n_0 and p_0 are the equilibrium electron and hole densities, and n_1 and p_1 are the equilibrium electron and hole densities when the Fermi level coincides with the Fe_i level. The sub-index 0 of the Fe_i concentrations is used to indicate the thermal-equilibrium condition.

In the previous model where $[\text{Fe}_i] \ll \text{doping}$, n_0 and p_0 can be easily determined using the doping concentration and

$$n_0 p_0 = n_i^2 \quad (2)$$

where n_i is the intrinsic carrier density. However, when the defect concentration becomes significant, the number of carriers arising from defect ionization is non-negligible. So the positively or negatively charged defects must be also included in the charge neutrality equation to determine n_0 and p_0 . In B- or P-doped Si

$$p_0 + [\text{Fe}_i^+]_0 + [\text{P}^+] = n_0 + [\text{B}^-] \quad (3)$$

It means that $[\text{Fe}_i^+]_0$ also acts as a donor dopant contributing to n_0 , just like $[\text{P}^+]$. With known $[\text{Fe}_i]$, we also have the mass conservation equation

$$[\text{Fe}_i^+]_0 + [\text{Fe}_i^0]_0 = [\text{Fe}_i] \quad (4)$$

Then, the four unknowns n_0 , p_0 , $[\text{Fe}_i^+]_0$, and $[\text{Fe}_i^0]_0$ can be solved with the four equations above.

2.2. Non-Equilibrium Steady State

Based on Shockley and Read's work,^[19] the expressions for the occupancy ratio and even the recombination lifetime of a monovalent defect are *not* affected by the assumption of the defect concentration. Those for a multivalent defect are not affected either, according to Sah and Shockley's work.^[21] The complication brought by a significant defect concentration is, as discussed by Shockley and Read, that the excess carrier densities Δn and Δp are no longer necessarily equal, due to the change in

Table 1. Energy levels E_t and electron/hole capture cross section ratios k of Fe_i^[35] and monatomic H^[1,16] in Si at 27 °C.

	E_t	k
Fe _i ^{0/+}	$E_v + 0.38 \text{ eV}$	188
H ^{0/+}	$E_c - 0.16 \text{ eV}$	1
H ^{-/0}	$(E_c + E_v)/2 - 0.064 \text{ eV}$	0.05

the occupied states at the defect level.^[19,28] For Fe_i, the general occupancy ratio is^[16]

$$\frac{[\text{Fe}_i^+]}{[\text{Fe}_i^0]} = \frac{kn_1 + p}{kn + p_1}; \quad n = n_0 + \Delta n, \quad \text{and} \quad p = p_0 + \Delta p \quad (5)$$

We can see that the occupancy ratio has changed from Equation (1) to (5) from the thermal equilibrium to the non-equilibrium steady-state condition. Here, a certain number of electrons (or holes) are emitted or captured by the defect atoms. This number is non-negligible when the defect concentration is significant, and can be only added to or taken from the excess carrier density Δn or Δp , because the equilibrium carrier densities n_0 and p_0 are deemed immutable by carrier injection. Note that, because all the equations in this work describe the system in the final steady state, both Δn and Δp are steady-state densities, instead of the injected/generated numbers at the beginning of the injection/generation event. Whether the steady-state density equals the injected density depends on whether the defect is a donor or an acceptor.

The charge neutrality equation in non-equilibrium steady state is

$$p + [\text{Fe}_i^+] + [\text{P}^+] = n + [\text{B}^-] \quad (6)$$

And we have another mass conservation equation

$$[\text{Fe}_i^+] + [\text{Fe}_i^0] = [\text{Fe}_i] \quad (7)$$

One of the excess carrier densities Δn and Δp must be given to specify the non-equilibrium condition, and the other is to be solved. This, plus $[\text{Fe}_i^+]$ and $[\text{Fe}_i^0]$, are three additional unknowns, and can be solved with Equation (5)–(7).

Overall, Equation (1)–(7) constitute a complete solution model for the seven important parameters describing the charge distribution of a monovalent defect, as well as the carrier densities in the conduction and valence bands in both thermal equilibrium and non-equilibrium steady state. For multivalent defects, one more energy level is associated with one more charge state. This adds two more unknown parameters: the defect concentration in the additional charge state in thermal equilibrium, and that in non-equilibrium steady state. Correspondingly, two more equations will be available to solve them: the occupancy ratio equation for the additional energy level in thermal equilibrium, and that in non-equilibrium steady state. Hence, the solution model can be generalized to multivalent defects with two or more energy levels. For the two-level monatomic H, the nine unknown parameters and nine equations are presented in the Appendix.

In the actual calculations in this work, temperature-dependent values of n_i , N_c , N_v , and E_g were calculated based on the parameterization by Couderc et al.^[33] The relative position of the defect levels were considered as temperature-independent.^[16] No pairing reactions between defects and dopants were considered, meaning that the stated Fe_i and H concentrations are all isolated atoms. Some of the modeling results shown in the following discussion may remain highly theoretical and unrealistic, especially when a rather high concentration of Fe_i or H is assumed to remain uniformly dissolved and isolated in Si at room temperature or slightly elevated temperatures. Nevertheless, the modeling

results serve the purpose of visualizing the physics, predicting the effects of defect concentration, temperature, and injection, and exemplifying potential applications of the model.

3. Results

Figure 1 shows the modeled charge distribution of Fe_i and p_0 in thermal equilibrium at 27 °C in p-Si, as functions of $[\text{Fe}_i]$. We have shown the doping level $[\text{B}^-] = 1 \times 10^{14} \text{ cm}^{-3}$ as a horizontal line, trying to visualize the charge neutrality equation

$$[\text{B}^-] - [\text{Fe}_i^+]_0 = p_0 \quad (8)$$

This is Equation (3) omitting $[\text{P}^+]$ and ignoring n_0 in p-Si. This relation can be understood in an intuitive way that, the B doping is compensated by the increasing active donors $[\text{Fe}_i^+]_0$, resulting in a decreasing net doping level p_0 , as visualized by the curves. Meanwhile, the Fermi level is dragged closer to the conduction band under this compensation effect, resulting in decreasing occupancy ratio $[\text{Fe}_i^+]_0/[\text{Fe}_i^0]_0$, as shown by the $[\text{Fe}_i^+]_0$ and $[\text{Fe}_i^0]_0$ curves.

Figure 2 shows the modeling results of the system in steady state under an injection of $\Delta p = 1 \times 10^{14} \text{ cm}^{-3}$. A very important relation visualized in this figure is

$$\Delta p - \Delta n = [\text{Fe}_i^+]_0 - [\text{Fe}_i^+] \quad (9)$$

It is obtained by subtracting the charge neutrality equations in thermal equilibrium (Equation (3)) and in non-equilibrium steady state (Equation (6)), again omitting $[\text{P}^+]$ and ignoring n_0 in p-Si. It directly describes how the equality between the excess hole and electron densities is disturbed by the change in the occupied states at the defect level. In a more intuitive way, under injection, a number of Fe_i⁺ atoms become neutral, by retrieving electrons from the injected electrons; consequently, Δn is deficient of Δp by the same number in the final steady state. In this case, the injected hole density equals the steady-state value Δp .

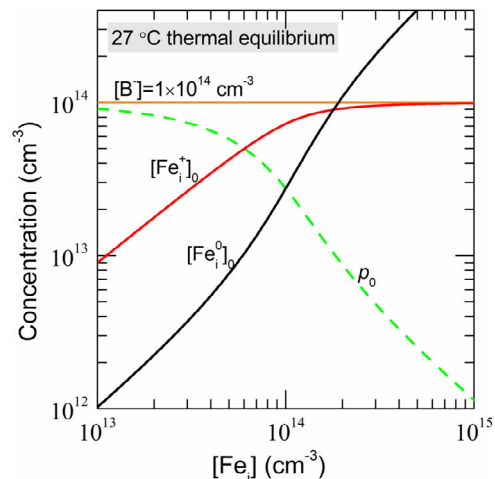


Figure 1. $[\text{Fe}_i^+]_0$, $[\text{Fe}_i^0]_0$, and p_0 in thermal equilibrium at 27 °C in Si with $[\text{B}^-] = 1 \times 10^{14} \text{ cm}^{-3}$, as a function of $[\text{Fe}_i]$.

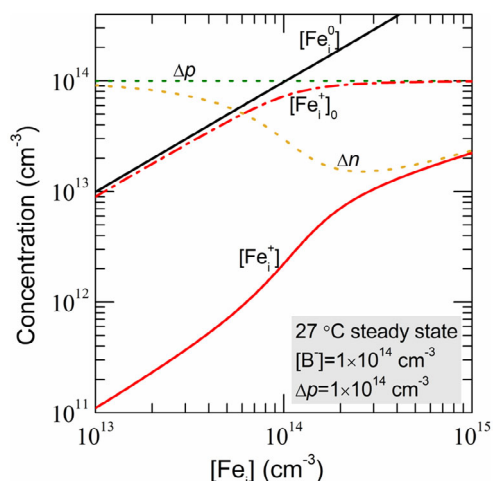


Figure 2. $[\text{Fe}_i^+]$, $[\text{Fe}_i^0]$, and Δn in steady state at 27 °C in Si with $[\text{B}^-] = 1 \times 10^{14} \text{ cm}^{-3}$ and $\Delta p = 1 \times 10^{14} \text{ cm}^{-3}$, as a function of $[\text{Fe}_i]$.

The modeled results of monatomic H in various conditions are shown in **Figure 3**. In 27 °C thermal equilibrium, H^+ is the dominant charge state in p-Si when the monatomic H concentration $[\text{H}] < [\text{B}^-]$, and compensates the B doping; H^- is the dominant charge state in n-type Si (n-Si), compensating the P doping. This compensation effect is more conspicuous in p-Si as shown by the results: the p-Si is converted to n-Si when $[\text{H}] > [\text{B}^-]$. This in return affects the Fermi level and thus the charge distribution dramatically, as shown in Figure 3a. A potential application of the model is for the hydrogen-containing heavily doped poly-Si layers, such as those shown in the SIMS results in Wenham et al.'s work.^[27] Low injection levels are always expected due to the heavy doping and low lifetime. The modeling results under such conditions will therefore very much resemble those in Figure 3a,b: dominant H^+ in p-Si and H^- in n-Si are expected when $[\text{H}]$ is lower; a higher $[\text{H}]$ exceeding the doping concentration may convert the doping type and result in a dramatic change in the charge distribution. These results might help explain the different firing stability

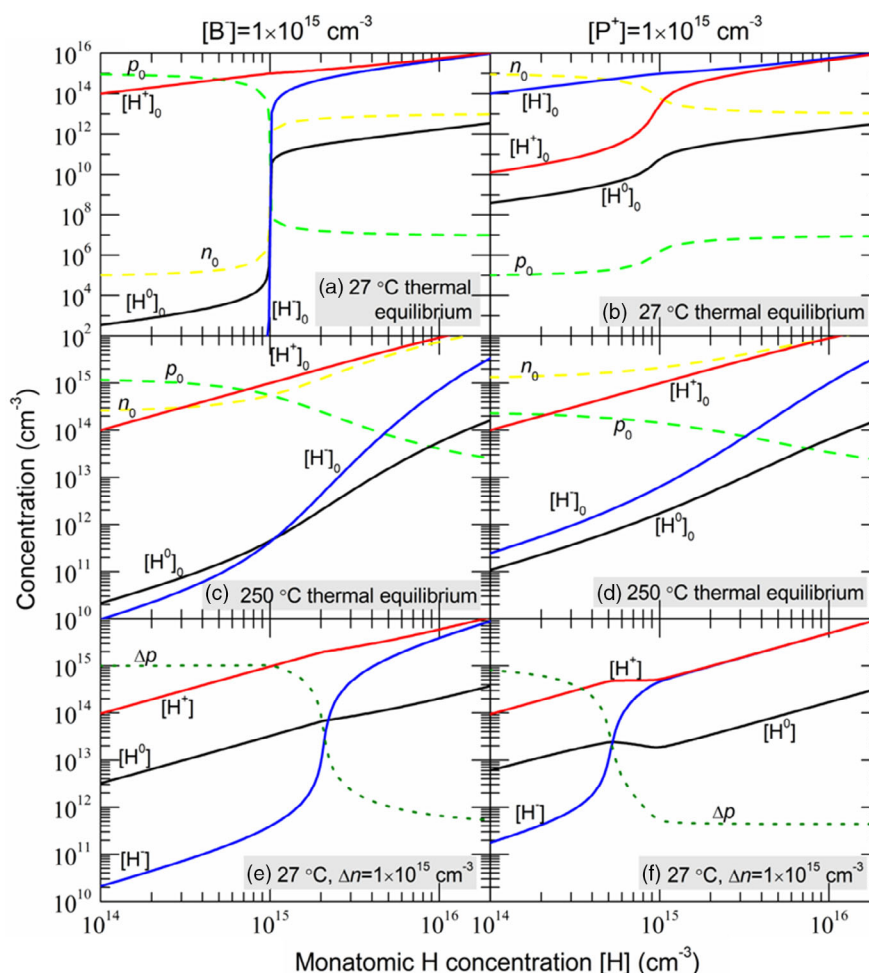


Figure 3. Carrier densities and charge distribution of monatomic H, as functions of the monatomic H concentration $[\text{H}]$, in (a,b) 27 °C thermal equilibrium, c,d) 250 °C thermal equilibrium, and e,f) 27 °C non-equilibrium steady state with $\Delta n = 1 \times 10^{15} \text{ cm}^{-3}$, in both p-Si with $[\text{B}^-] = 1 \times 10^{15} \text{ cm}^{-3}$ (a,c,e), and n-Si with $[\text{P}^+] = 1 \times 10^{15} \text{ cm}^{-3}$ (b,d,f).

of n- and p-type heavily doped poly-Si observed in a previous study.^[34]

Less difference between n- and p-Si is observed when the temperature is elevated to 250 °C. H^+ becomes the dominant charge state in both types of Si: it compensates the p-type doping in p-Si, converting p-Si to n-Si when $[H] > [B^-]$, but enhances the n-type doping in n-Si. Under an injection level of $\Delta n = 1 \times 10^{15} \text{ cm}^{-3}$ in steady state at 27 °C, H^+ is still the dominant charge state in both types of Si. Note that the results of n_0 and p_0 in Figure 3e,f remain the same as those in Figure 3a,b, and were thus not plotted twice. It can be observed that the fraction of H^0 is increased by both an elevated temperature and carrier injection in both types of Si. The same trends were also predicted by the previous model for lower $[H]$.^[16] As H^0 is usually considered to be much more mobile than the charged species H^+ and H^- , strategies for achieving better hydrogenation effects in Si were developed based on this prediction.^[3,4,23]

4. Conclusions

A rigorous methodology for modeling the charge state of monatomic H and other defects with arbitrary concentrations in Si is presented. In comparison with the charge state model described in our previous work,^[16] the assumption that the defect concentration is much lower than the doping level is avoided in the new model. We have shown that, the general occupancy ratio from the previous model can still be applied to the charge state prediction of mono-/multivalent and in thermal equilibrium/non-equilibrium steady-state conditions, without any change in the expression $\alpha = (kn_1 + p)/(kn + p_1)$, even when the defect concentration is significant. The complication induced by avoiding the previous assumption mainly lies in calculating the equilibrium and excess carrier densities which are required in the occupancy ratio, because of 1) the non-negligible contribution to n_0 and p_0 from defect ionisation, and 2) unequal Δn and Δp caused by the change in the occupied states at the defect level from equilibrium to non-equilibrium. The two effects can be completely and conveniently accounted for by the charge neutrality equations in thermal equilibrium and non-equilibrium steady state. For a monovalent defect, the model consists of 7 equations, to solve the 7 required parameters of the charge distribution and carrier densities. For multivalent defects, 1 additional energy level adds 2 additional parameters and 2 additional equations. The model was applied to Fe_i and monatomic H in Si, where the effects of defect concentration, temperature, and carrier injection on the charge distribution and carrier densities were modeled and discussed.

Appendix: Charge State Prediction Model for Monatomic H in Si

There are in total 9 unknown parameters to be solved: n_0 , p_0 , one of Δn and Δp (the other one is known), $[H^+]_0$, $[H^0]_0$, $[H^-]_0$, $[H^+]$, $[H^0]$, and $[H^-]$. In accordance, nine equations are given as follows.

The occupancy ratios at the donor and the acceptor levels of H in thermal equilibrium are

$$\frac{[H^+]_0}{[H^0]_0} = \left(\frac{v_+ Z_+}{v_0 Z_0} \right) \cdot \frac{p_0}{p_d} \quad (A1)$$

$$\frac{[H^0]_0}{[H^-]_0} = \left(\frac{v_0 Z_0}{v_- Z_-} \right) \cdot \frac{p_0}{p_a} \quad (A2)$$

The occupancy ratios in nonequilibrium steady state are

$$\frac{[H^+]}{[H^0]} = \left(\frac{v_+ Z_+}{v_0 Z_0} \right) \cdot \frac{k_d n_d + p}{k_d n + p_d} \quad (A3)$$

$$\frac{[H^0]}{[H^-]} = \left(\frac{v_0 Z_0}{v_- Z_-} \right) \cdot \frac{k_a n_a + p}{k_a n + p_a} \quad (A4)$$

where $n = n_0 + \Delta n$ and $p = p_0 + \Delta p$; k_d and k_a are the electron/hole capture cross-section ratios of the donor level and the acceptor level, respectively; n_d and p_d are the equilibrium electron and hole densities when the Fermi level coincides with the donor level, and n_a and p_a are those for the acceptor level. The energy levels and capture cross section ratios of H can be found in Table 1. The spin degeneracy of monatomic H is considered in the model based on Herring et al.'s work,^[1] via two parameters $-v_s$, the number of possible sites or orientations per unit cell, and Z_s , the effective partition function of the charge state s . Their values used in this work are from Herring et al.'s work^[1]: $v_0 = 8$, $v_+ = 4$, $v_- = 2$, and $Z_s = 1$.

In B- or P-doped Si, the charge neutrality equations in thermal equilibrium and non-equilibrium steady state are

$$p_0 + [H^+]_0 + [P^+] = n_0 + [H^-]_0 + [B^-] \quad (A5)$$

$$p + [H^+] + [P^+] = n + [H^-] + [B^-] \quad (A6)$$

The mass conservation of H in thermal equilibrium and non-equilibrium steady state

$$[H^+]_0 + [H^0]_0 + [H^-]_0 = [H] \quad (A7)$$

$$[H^+] + [H^0] + [H^-] = [H] \quad (A8)$$

And at last

$$n_0 p_0 = n_i^2 \quad (A9)$$

Acknowledgements

This work was supported by the Australian Renewable Energy Agency (ARENA) through projects RND 005 and 1-A060. C.S. is supported by an Australian Centre for Advanced Photovoltaics (ACAP) Postdoctoral Research Fellowship.

Conflict of Interest

The authors declare no conflict of interest.

Data Availability Statement

The data that support the findings of this study are available from the corresponding author upon reasonable request.

Keywords

charge states, crystalline silicon, hydrogen, hydrogenation, recombination, Shockley–Read–Hall model

Received: September 9, 2021

Revised: September 20, 2021

Published online: October 13, 2021

- [1] C. Herring, N. Johnson, C. G. Van de Walle, *Phys. Rev. B* **2001**, 64, 125209.
- [2] V. V. Voronkov, R. Falster, *Phys. Status Solidi B* **2017**, 254, 1600779.
- [3] P. Hamer, B. Hallam, S. Wenham, M. Abbott, *IEEE J. Photovoltaics* **2014**, 4, 1252.
- [4] P. Hamer, B. Hallam, R. S. Bonilla, P. P. Altermatt, P. Wilshaw, S. Wenham, *J. Appl. Phys.* **2018**, 123, 043108.
- [5] S. Leonard, V. Markevich, A. Peaker, B. Hamilton, *Appl. Phys. Lett.* **2013**, 103, 132103.
- [6] S. Leonard, V. Markevich, A. Peaker, B. Hamilton, J. Murphy, *Appl. Phys. Lett.* **2015**, 107, 032103.
- [7] J. Mullins, V. P. Markevich, M. P. Halsall, A. R. Peaker, *Phys. Status Solidi A* **2016**, 213, 2838.
- [8] J. Mullins, S. Leonard, V. Markevich, I. Hawkins, P. Santos, J. Coutinho, A. Marinopoulos, J. Murphy, M. Halsall, A. Peaker, *Phys. Status Solidi A* **2017**, 214, 1700304.
- [9] J. Mullins, V. Markevich, S. Leonard, M. Halsall, A. Peaker, *ECS Trans.* **2018**, 86, 125.
- [10] J. Mullins, V. P. Markevich, M. P. Halsall, A. R. Peaker, *Phys. Status Solidi A* **2019**, 216, 1800611.
- [11] C. Sun, A. Liu, S. P. Phang, F. E. Rougieux, D. Macdonald, *J. Appl. Phys.* **2015**, 118, 085709.
- [12] H. Reiss, C. Fuller, F. Morin, *Bell Labs Techn. J.* **1956**, 35, 535.
- [13] L. Kimerling, J. Benton, *Phys. B+ C* **1983**, 116, 297.
- [14] H. Conzelmann, K. Graff, E. Weber, *Appl. Phys. A* **1983**, 30, 169.
- [15] C. Sun, Y. Zhu, M. Juhl, W. Yang, F. Rougieux, Z. Hameiri, D. Macdonald, *Phys. Status Solidi RRL*, <https://doi.org/10.1002/pssr.202000520>.
- [16] C. Sun, F. E. Rougieux, D. Macdonald, *J. Appl. Phys.* **2015**, 117, 045702.
- [17] F. E. Rougieux, C. Sun, D. Macdonald, *Sol. Energy Mater. Sol. Cells* **2018**, 187, 263.
- [18] W. Shockley, J. Last, *Phys. Rev.* **1957**, 107, 392.
- [19] W. Shockley, W. Read Jr, *Phys. Rev.* **1952**, 87, 835.
- [20] R. N. Hall, *Phys. Rev.* **1952**, 87, 387.
- [21] C.-T. Sah, W. Shockley, *Phys. Rev.* **1958**, 109, 1103.
- [22] P. Landsberg, *Proc. Phys. Soc. Sect. B* **1957**, 70, 282.
- [23] B. J. Hallam, P. G. Hamer, S. R. Wenham, M. D. Abbott, A. Sugianto, A. M. Wenham, C. E. Chan, G. Xu, J. Kraiem, J. Degoulange, *IEEE J. Photovoltaics* **2014**, 4, 88.
- [24] P. Würfel, U. Würfel, *Physics of Solar Cells: From Basic Principles to Advanced Concepts*, John Wiley & Sons, New York **2009**.
- [25] S. Kleekajai, F. Jiang, M. Stavola, V. Yelundur, K. Nakayashiki, A. Rohatgi, G. Hahn, S. Seren, J. Kalejs, *J. Appl. Phys.* **2006**, 100, 093517.
- [26] D. C. Walter, D. Bredemeier, R. Falster, V. V. Voronkov, J. Schmidt, *Sol. Energy Mater. Sol. Cells* **2019**, 200, 109970.
- [27] A. Cielsa née Wenham, S. Wenham, R. Chen, C. Chan, D. Chen, B. Hallam, D. Payne, T. Fung, M. Kim, S. Liu, in *2018 IEEE 7th World Conf. on Photovoltaic Energy Conversion (WCPEC) (A Joint Conf. of 45th IEEE PVSC, 28th PVSEC & 34th EU PVSEC)*, IEEE, Piscataway, NJ, USA **2018**, pp. 0001–0008; <https://doi.org/10.1109/PVSC.2018.8548100>.
- [28] J. Blakemore, *Semiconductor Statistics*, Pergamon Press, Oxford, UK **1962**.
- [29] R. Chen, A. M. Ciesla, D. Chen, C. E. Chan, P. G. Hamer, B. J. Hallam, S. R. Wenham, in *2018 IEEE 7th World Conf. on Photovoltaic Energy Conversion (WCPEC) (A Joint Conf. of 45th IEEE PVSC, 28th PVSEC & 34th EU PVSEC)*, IEEE, Piscataway, NJ, USA **2018**, pp. 0053–0057; <https://doi.org/10.1109/PVSC.2018.8548195>.
- [30] K. R. McIntosh, B. B. Paudyal, D. H. Macdonald, *J. Appl. Phys.* **2008**, 104, 084503.
- [31] A. Istratov, H. Hieslmair, E. Weber, *Appl. Phys. A* **1999**, 69, 13.
- [32] C. G. Van de Walle, J. Neugebauer, *Annu. Rev. Mater. Res.* **2006**, 36, 179.
- [33] R. Couderc, M. Amara, M. Lemiti, *J. Appl. Phys.* **2014**, 115, 093705.
- [34] D. Kang, H. C. Sio, J. Stuckelberger, D. Yan, H. T. Nguyen, T. N. Truong, R. Liu, D. Macdonald, in *2021 IEEE 48th Photovoltaic Specialists Conf. (PVSC)*, IEEE, Piscataway, NJ, USA **2021**, pp. 0701–0705; <https://doi.org/10.1109/PVSC43889.2021.9519080>.
- [35] D. Macdonald, J. Tan, T. Trupke, *J. Appl. Phys.* **2008**, 103, 073710.